

CO3-1 Development on In-reactor Observation System Using Cherenkov Light (II)

N. Takemoto, K. Tsuchiya, Y. Nagao, S. Kitagishi, M. Naka, A. Kimura, T. Sano¹, H. Unesaki¹, T. Yoshimoto¹, K. Nakajima¹, Y. Fujihara¹ and K. Okumura¹

Neutron Irradiation and Testing Reactor Center, JAEA
¹Research Reactor Institute, Kyoto University

INTRODUCTION: The Cherenkov light is a faint emission accompanying the passage of charged particles through a transparent medium at speeds faster than the speed of light in that medium [1]. Last year, the observation system of Cherenkov light was developed and preliminary tests were carried out with the halogen light [2]. In this study, Cherenkov light was observed by this system during KUR operation and the effect on transmittance of change of the diaphragm and ND-filters was investigated.

EXPERIMENTS: As the first experiment, the illuminance of Cherenkov light was measured by the digital illuminance meter (IM-5, TOPCON) during KUR operation. This meter was fixed by the jig and installed in the pipe for observation hole. The neutral density filters (ND-filters) were changed during the observation of Cherenkov light.

As the second experiment, Cherenkov light was observed by the observation system (Fig.1 in ref. [2]). The camera of observation system was fixed by the jig and installed in the pipe for core observation hole. The change of the diaphragm and ND-filters were carried out during the observation of Cherenkov light. After the observation, the obtained data were evaluated by the image processing software called “Image J”.

RESULTS: The relationship of transmittance between the catalogue value and measured value of the ND-filters is shown in Fig.1. The illuminance with no ND-filter was 0.230 lx and these values were corrected by the angle of

incidence. From the result, the transmittance of Cherenkov light was almost the same tendency as that of the halogen light and the effect on the transmittance of the ND-filters was the same as that of the catalogue value.

The analysis of Cherenkov light was carried out with the fuel element in the “Ho-6”. The analysis result by the Image J is shown in Fig.2. The relative intensity of light decreased with increasing the diaphragm number. In Fig.2, the change of transmittance was evaluated at the points (a) and (b). The relationship of transmittance between the calculated value and measured value of the diaphragm is shown in Fig.3. Here, the calculated values were determined to raise the rate of the diaphragm numbers to the second power and the measured values were calculated by the analysis results. From the result, the measured values did not agree with the calculated values in the range of high transmittance. On the other hand, the transmittance with ND-0.9 filter is a half of that with ND-0.6 filter. However, the transmittances between ND-0.6 and 0.9 were about 70 and 51% at the diaphragms of F1.8 and F2.8, respectively. In future, it is necessary to evaluate this phenomenon including the halation and evaluation procedure by “Image J”.

CONCLUSION: The measurement of Cherenkov light was carried out with the observation system. Correlation between illuminance of Cherenkov light and ND-filter was evaluated and the transmittance of Cherenkov light almost agreed with the catalogue value. On the other hand, the transmittance with ND-filter and diaphragm by the camera was different from the calculated values. The measuring and analysis procedures will be improved in future.

REFERENCES:

- [1] J.V. Jelley, Cherenkov Radiation and its Applications (Pergamon, New York, 1958).
- [2] K. Tsuchiya, S. Kitagishi, et al., KURR Progress Report, (2009) p.196.

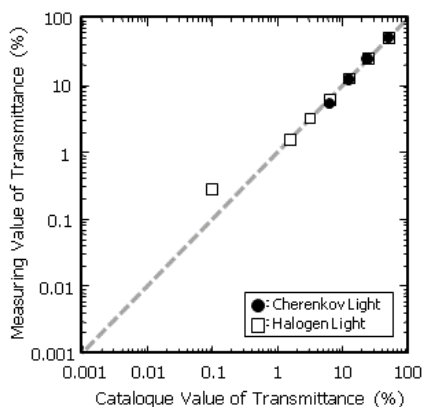


Fig.1. Relationship of transmittance between the catalogue value and measuring value of ND-filters.

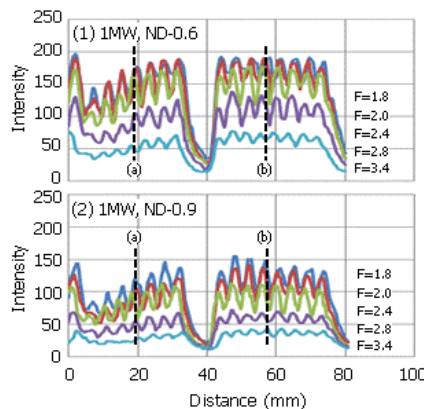


Fig.2. Analysis of Cherenkov light in the fuel element in the “Ho-6”.

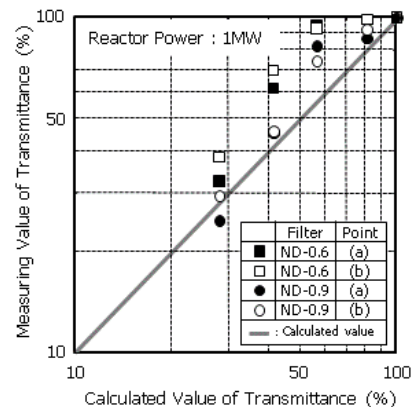


Fig.3. Relationship of transmittance between the calculated value and measured value with the Image J.

CO3-2 Development of Subcriticality Measurement for Accelerator-Driven Reactor (V)

K. Hashimoto, W. Sugiyama, A. Sakon¹, S. Tomizuka¹, A. Matsumoto¹, C. Pyeon², T. Misawa², T. Sano², H. Nakamura² and H. Unesaki²

Atomic Energy Research Institute, Kinki University
¹Interdisciplinary Graduate School of Science and Technology, Kinki University
²Research Reactor Institute, Kyoto University

INTRODUCTION: An accelerator-driven subcritical reactor system has been constructed in A-loading facility of the KUCA and a series of power spectrum measurement and Feynman- \square analyses have been performed to develop the methodology of these subcriticality measurements. The preliminary results of power spectrum measurements are showed in this report.

EXPERIMENTS: These measurements were performed in a reactor system referred to as A3/8”P36EU (3). A tritium target was placed outside polyethylene reflector and pulsed neutron beam was emitted from the target. As pulsed beam frequency, 20, 100 and 500Hz were employed. Coherence function between two BF₃ counters closely placed were measured to determine the prompt-neutron decay constant. The experiments were carried out in two subcritical states. The subcriticality of the state was adjusted by changing control rod pattern. These control rod patterns are showed in Table 1.

Table 1. Control rod patterns employed

Pattern	Rod Position			Reactivity [%Δk/k]
	C1	C2, C3	S4-S6	
B	L.L.	L.L.	U.L.	-0.636
C	L.L.	L.L.	L.L.	-1.577

L.L.: Lower Limit, U.L.: Upper Limit

RESULTS: Figure 1 shows a cross-power spectral density measured in a subcritical system (rod pattern B) driven by pulsed source, whose repetition frequency is 20Hz. The spectral density consists of a continuous reactor-noise component and many delta-function-like peaks at integral multiple of the repetition frequency (20Hz). In the figure, a least-squares fit of the following equation to the data of continuous component is also shown:

$$\Phi(\omega) = \frac{A}{\alpha^2 + \omega^2}, \quad (1)$$

where the point data of delta-function-like peaks are masked. No systematic deviation of the fitted curve from the data of continuous component can be seen.

Figure 2 shows another least-squares fit of the above equation to the point data of delta-function-like peaks, where the other data, i.e., the data of continuous component are masked. No systematic deviation of the fitted

curve from the point data can be also observed.

The prompt-neutron decay constants α inferred from cross-power spectral density are summarized in Table 1. The present decay constant is consistent with that obtained by a pulsed neutron experiment [1].

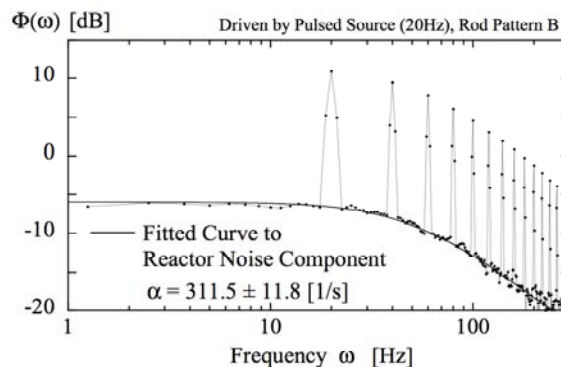


Fig.1. Least-squares fit to continuous reactor-noise component of cross-power spectral density (pulse repetition frequency of 20Hz)

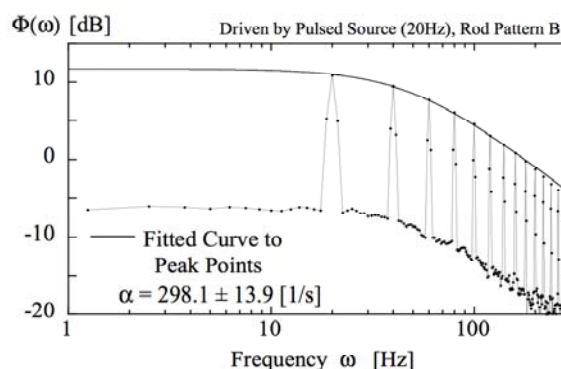


Fig.2. Least-squares fit to peak points of cross-power spectral density (pulse repetition frequency of 20Hz).

Table 1. Prompt-neutron decay constant (Rod Pattern B)

Pulse Repetition Frequency [Hz]	Prompt-Neutron Decay Constant α [1/s]	
	Present Spectral Analysis	Pulsed Neutron Experiment
-----	326.1 ± 14.6	
20	311.5 ± 11.8	
100	298.1 ± 13.9	303.9 ± 2.8
500	308.9 ± 15.9	
-----	327.4 ± 11.1	

----- Driven by Am-Be Source

REFERENCES:

[1] H. Taninaka, K. Hashimoto, C. Pyeon, T. Sano, T. Misawa and T. Ohsawa, *J. Nucl. Sci. Technol.*, **47** (2010) 376-383.

CO3-3 Measurements of Reactivity Worth of Rare-Earth Elements (II)

K. Shimozato, K. Ieyama, T. Kitada and H. Unesaki¹

Graduate School of Engineering, Osaka University
¹Kyoto University Research Reactor Institute

INTRODUCTION: Rare-earth elements are considered as a candidate of advanced burnable poison. However, few critical experiments have been carried out so far to validate the accuracy of their nuclear data. So critical experiments loaded with rare-earth elements (Dy, Ho, Er and Tm) were carried out and their reactivity worth were measured at the KUCA B core in 2009. However there are relatively large deviations in measured reactivity worth. Therefore the object of this experiment is to reduce the deviation by increasing the number of measurements, and also to evaluate the accuracy of cross section data of the rare-earth elements in detail.

EXPERIMENTS: The experiments were performed at two kinds of assemblies named B3/8”P36EU(3) and B1/8”P60EU-EU(5) where neutron spectra are different each other. There are four elements to be measured: dysprosium (Dy), holmium (Ho), erbium (Er) and thulium (Tm). The rare-earth elements were used in the oxide form in the experiment and they were packed into an Al sample case (50.8mm × 50.8mm × 10.0mm). Measured samples are the same those used in the last year. The Al sample case was inserted at the center of fuel element (“sample fuel element”) as shown in Fig.1.

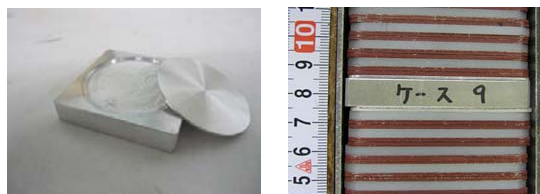


Fig.1. The packing of rare-earth elements (left): the loading of Al sample case to sample fuel element (right).

The sample fuel element was loaded at the center of the core as shown in Fig.2. Figure 2 shows the arrangement of the two cores to be measured the sample worth. Two kinds of cores with different neutron spectrum (the B3/8”P36EU (3) core (E3 core) - softer spectrum, the B1/8”P60 EU-EU (5) core (EE1 core)- harder spectrum) were constructed to obtain the dependency of the sample worth on the neutron spectrum. The evaluation of sample worth was performed by measuring the change in excess reactivity caused by the change of Al sample cases with/without rare-earth sample. The excess reactivity of the core without rare-earth sample is measured many times to reduce the deviation during the experiment. These data are depicted in Fig.3 with measured data in 2009 in the order of measured date. The excess reactivity varies and the range of variation is too wide (around

0.09% $\Delta k/k$) compared to the target sample worth of 0.15% $\Delta k/k$. Therefore the experiments were performed especially to be clear the reason why and what causes the change in excess reactivity with the aid of simulations of MVP which is the continuous energy Monte Carlo code.

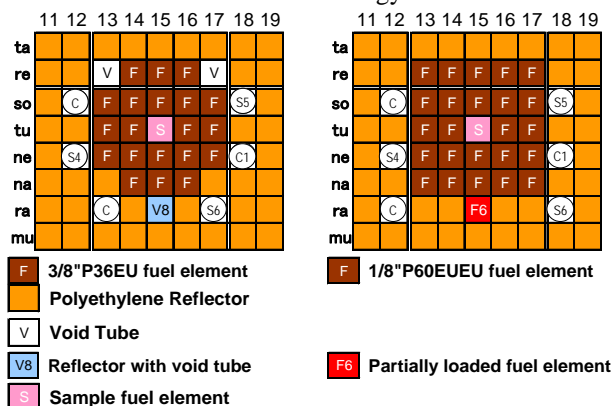


Fig.2. Arrangement of the two cores (left- E3 core, right- EE1 core).

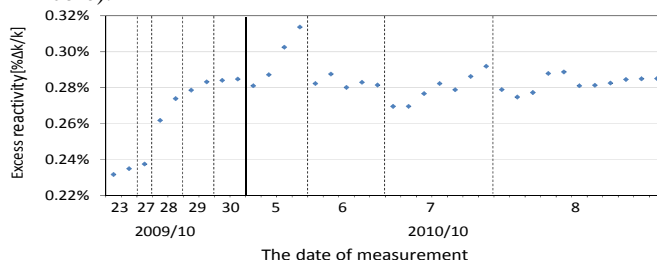


Fig.3. Measured excess reactivity of EE1 core without rare-earth sample.

There are some reasons as the cause of the variation: the accuracy of re-construction of “sample fuel element” by replacing Al cases, of movable center core, and of the position of control rod to achieve the critical point were considered and measured in the experiment. As the results the variation caused by “sample fuel element” is negligibly small because of the fact that the upper vacant length of sample fuel element is not changed in each replacement of sample, and also standing in stable state in a week, and center core causes around 0.2% $\Delta k/k$ and the position of CR causes less than 0.01% $\Delta k/k$. There are other causes to be considered but we could not consider any more now, and this is the future work in the future.

RESULTS: The deviation of sample worth of the rare-earth elements became smaller than before by increasing the number of measurements and the validity of cross section of the elements are confirmed more accurately. Although it was found that the variation of measured excess reactivity is caused by many variations such as the position of the center core and control position, the further investigation is to be needed to be clear the major cause of the variation.

CO3-4 Development of Measurement Technique of Thermal Neutron Directional Distributions in a Nuclear Reactor Using a Compact Directional Neutron Sensor

K. Watanabe, S. Maruyama, A. Uritani, A. Yamazaki, C. Pyon¹ and T. Misawa¹

Graduate School of Engineering, Nagoya University
¹Research Reactor Institute, Kyoto University

INTRODUCTION: Computer simulation plays an important role for design of new type reactors. Validity of calculation results should be confirmed through basic experiments. By recent remarkable progress of calculation performance, some differential information, such as a neutron spectrum and a neutron directional distribution, can also be calculated. However, since these differential information are generally difficult to be measured in experiments, integrated information, such as the reaction rate of an activation foil, are compared with calculation results. We, therefore, have developed a novel compact directional neutron sensor for measurement of thermal neutron directional distribution in a nuclear reactor.

A conceptual drawing of the compact directional neutron sensor is shown in Fig. 1. This sensor consists of a Eu:LiCaAlF₆ scintillator for thermal neutron detection, thermal neutron shielding made of a silicon rubber including gadolinium oxide powder, a light guide for transmission of the scintillation photons and a photomultiplier tube. The neutron shielding has a slit to collimate thermal neutrons. Since only thermal neutrons passing through the slit can be detected, the sensor has a directional response. To prevent neutrons from coming into the scintillator through the light guide, a transparent crystal including lithium, *i.e.* non-doped LiCaAlF₆, is inserted. The whole sensor can be rotated by using a remote controllable rotary actuator.

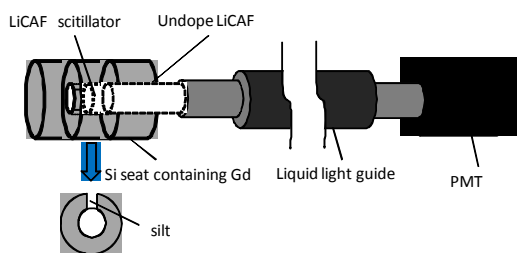


Fig. 1. A conceptual drawing of the compact directional neutron sensor.

PERFORMANCE EVALUATION: The angular resolution of this measurement system of thermal neutron directional distributions was evaluated through Monte Carlo simulations using Particle and Heavy Ion Transport

code System (PHITS). Fig. 2, shows the directional response of the measurement system for a parallel thermal neutron beam. The angular resolution was evaluated to be 30 degrees.

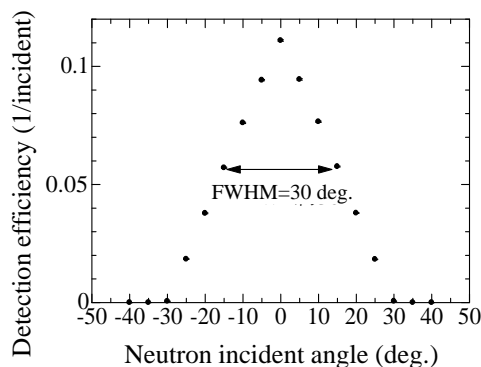


Fig. 2. The directional response of the measurement system of thermal neutron directional distributions using the compact directional neutron sensor.

EXPERIMENTS: We measured the thermal neutrons directional distribution in the A-core at the KUCA. Fig. 3, shows the directional distribution measured by the compact neutron directional sensor. The sensor was located at 15 cm far from the core surface. The direction to the core center is defined as 0 degrees. The sensor outputs are normalized by the fission chamber output. Two peaks that corresponded to the neutron streaming through narrow gaps of the polyethylene moderators were observed at about ± 45 degrees.

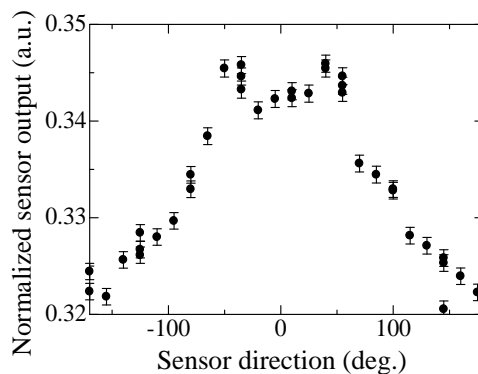


Fig. 3. The thermal neutron directional distribution in the A-core at the KUCA measured by the compact neutron directional sensor.

CO3-5 Quantification of Neutron and γ Ray Fields for Subcriticality Determination (III)

Y. Nauchi, T. Kameyama, H. Unesaki¹, T. Misawa¹
T. Sano¹ and T. Yagi²

Central Research Institute of Electric Power Industry

¹Research Reactor Institute, Kyoto University

²Graduate School of Energy Science, Kyoto University

INTRODUCTION: Quantification of neutron leakage from spent fuel assemblies is a promising measure for burn-up credit (BUC) application to transport and storage of them. Focusing that about 99% of leakage neutrons are absorbed by H(n, γ) reactions followed by emission of 2.223MeV γ rays, experimental studies had been conducted on measurements of the γ rays. In the previous study in 2009, we had succeeded in counting of the γ rays with a NaI detector set in water outside the core (Fig. 1). However, the ratios of γ rays from region of interest (ROI) to total ones, R , were around 60%. For BUC, R should be close to 100% to reduce errors originated in calculation of R s based on an assumed nuclide composition of a target assembly. For the purpose, measurements in new geometries were performed

EXPERIMENTS: 3 subcritical cores of 2 columns x 2, 3, 4 rows of C-35 fuel assemblies were mocked up in KU-CA-C core tank. The longer side of the assemblies was set to x axis. Moderator water level was down to 41cm above the bottom of the fuel. The NaI detector was lifted up by 9.7cm above the water surface. The subcritical cores were driven by a ²⁵²Cf source located near the center of them and 2.223MeV γ rays were measured by the detector. Distribution of thermal neutron flux $\phi_h(\mathbf{r})$ in ROI was measured in x and y axes with ⁶Li fiber scintillators and in z axis with activation of Indium wires. Such radiation measurements were also done for the source located in water without fuels.

DATA PROCESSING: The transport efficiency $\varepsilon(\mathbf{r})$ is determined by attenuation and the solid angle of the NaI to position \mathbf{r} . Average counting efficiency E over ROI is

$$E = \int_{\text{ROI}} \varepsilon(\mathbf{r}) \Sigma_a \phi(\mathbf{r}) d\mathbf{r}^3 / \int_{\text{ROI}} \Sigma_a \phi(\mathbf{r}) d\mathbf{r}^3.$$

E can be calculated assuming similarity of H(n, γ) reaction distribution $\Sigma_a \phi(\mathbf{r})$ to that of measured $\phi_h(\mathbf{r})$ in water outside the core. No information about fuel composition was used to deduce E . With count rate of 2.223MeV γ ray in the NaI, D , the number of neutron absorption in ROI,

A is derived as

$$AH = DR/E$$

using H , which is neutron absorption ratio in hydrogen to that in water. A_{Cf} for the geometry without fuel corresponds to source intensity S of ²⁵²Cf where $R_{Cf}=1.0$. For geometry i , we deduced $(A/S)_{pre,i}$ assuming $R_i=1$.

$$(A/S)_{pre,i} = (D_i/E_i)/(D_{Cf}/E_{Cf})$$

RESULTS: E and $(A/S)_{pre,i}$ are summarized in table 1. In 2010, difference of E s over cores is reduced by the new geometries. The E s increases in 2010 because of decrement of attenuation of γ rays in water around the NaI detector. Whereas, $(A/S)_{pre,i}$ decreases due to decrement of neutron multiplication by that of level of moderator. We calculated number of 2.223MeV pulse height counted in the NaI detector with MCNP-5, as well as R_i . Owing to the new geometry, R is raised by 17% on average. Although experimental data $(A/S)_{pre,i}$ are about 20% larger than $(A/S)_{calc,i}$, the discrepancy is improved by taking R_i into account. Finally deduced experimental value

$$(A_i/S)_{exp} = R_i (A_i/S)_{pre}$$

agrees with $(A/S)_{calc,i}$ within accuracy of 7%. Accordingly, the quantification of leakage neutrons by the measurement of H(n, γ) γ rays is promising for BUC application.

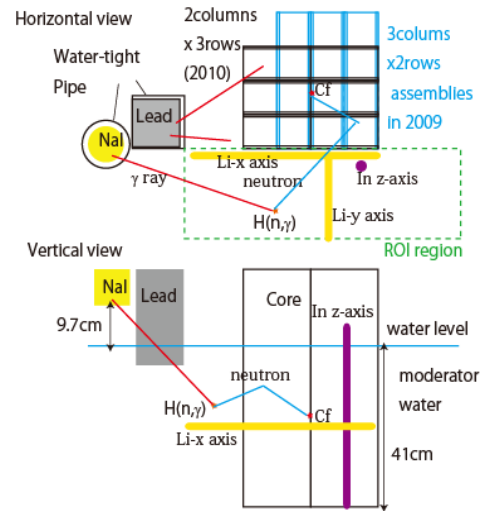


Fig.1. Geometry of H(n, γ) γ ray measurement.

Table 1: Summary of H(n, γ) γ ray measurement to quantify neutron leakage.

Fiscal year	assembly		E based on measurement	measured $(A/S)_{pre,i}$	calculated $(A/S)_{calc,i}$	$\frac{(A/S)_{calc,i}}{(A/S)_{pre,i}}$	calculated R	Final $(A/S)_{exp,i}$	$\frac{(A/S)_{calc,i}}{(A/S)_{exp,i}}$
	long side	column row							
2009	y axis	1.5 2	1.18E-05	0.683	0.429	0.628	0.623	0.426	1.008
	y axis	2 2	1.17E-05	0.799	0.490	0.614	0.594	0.474	1.033
	y axis	3 2	9.92E-06	1.553	1.090	0.702	0.654	1.016	1.073
	y axis	4 2	1.43E-05	3.722	2.670	0.717	0.679	2.527	1.057
2010	x axis	2 2	2.07E-05	0.633	0.559	0.883	0.841	0.533	1.049
	x axis	2 3	2.04E-05	1.015	0.845	0.832	0.805	0.817	1.033
	x axis	2 4	2.10E-05	1.396	1.141	0.818	0.763	1.065	1.072

T. Usui, S. Mikami, M. Hashimoto, N. Nakayama, C. Suzuki¹, K.Tani¹, K. Yamasaki² and T. Misawa²

H&S Division, O-arai Research and Development Center, JAEA

¹School of Engineering, The University of Tokyo

²Research Reactor Institute, Kyoto University

INTRODUCTION:

A composite-gas-filled proportional counting tube (hereinafter referred to as ‘CPCT’) for neutron dosimetry has been developed. This CPCT intend to estimate the conversion coefficient to H*(10) from thermal neutron flux based upon ratio of reactions to fast and thermal neutrons. The dosimetric functions of the CPCT have been confirmed by monoenergetic neutrons and leakage neutron spectrum from reactor vessels and fuel fabrication lines [1-2]. However, for the neutron dosimetry of accelerator-driven reactors, it is necessary to confirm further adaptability of the CPCT. A unique mix field of fast and thermal neutrons produced by Accelerator Driven Subcritical Reactor which driven by neutrons D-T reaction-origins were used. Therefore, in this year, experimental data of the CPCT measuring in core A of Kyoto University Critical Assembly (hereinafter referred to as KUCA) is collected.

EXPERIMENTS:

For acquiring the conversion coefficient of the CPCT, measurements with the CPCT were conducted in the stage next to the core A of KUCA, in the stage next to the accelerator and in the rotary shield room with a drive of core A. For measurement points of the stage next to the core A and the rotary shield room, measurements were conducted twice while changing the conditions of the reflector around the reactor.

The neutron energy spectra of those points were measured using the Bonner-ball method.

RESULTS:

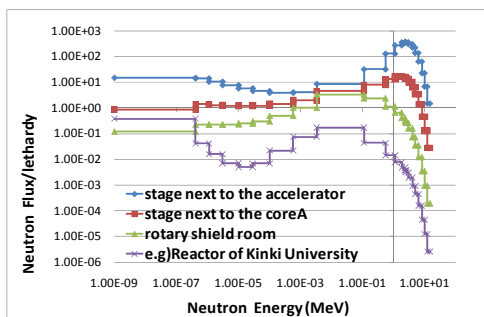


Fig.1. Neutron energy spectra evaluated by Bonner-ball method.

The neutron energy spectra of each measured point are shown in Fig.1.

The neutron energy is higher than leakage neutron spectrum from reactor vessels and fuel fabrication lines collected in the past as shown in Fig.1.

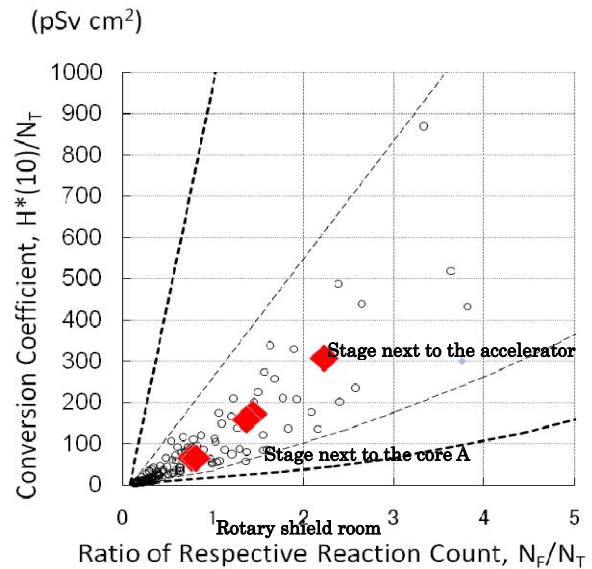


Fig. 2. Experimental results plotted in the convex hull

- - : Basal convex hull
- - - : Contracted convex hull
- ◆ : Experimental results in KUCA
- : Other Results(Experiment and calculation)

Fig. 2 shows experimentally evaluated conversion coefficient to H*(10) as a function of ratio of respective reaction counts of fast and thermal neutrons

All the plots are settled in the convex hull and the area in convex hull is closed up to the high group of ratio of fast neutron count.

Even if the condition of the reflector around the reactor and reactor power were different in core A of KUCA, a relationship between fast neutron / thermal neutron and conversion coefficient H*(10) / thermal neutron was roughly proportioned as shown in Fig.2.

A calculation accuracy of the conversion factor of the CPCT can be improved because the data was acquired in the unique field with a ratio of fast and thermal neutron.

REFERENCES:

[1] M. Hashimoto *et al.*, Radiat. Prot. Dosimetry, **136**(1) (2009) 1-10.
 [2] M. Hashimoto, Ph.D. Thesis, The University of Tokyo (2009)